ELSEVIER

Biophysical Chemistry 53 (1994) 85–94

Biophysical Chemistry

Small angle neutron scattering studies of structural characteristics of agarose gels

Susan Krueger [a], Anna Ploplis Andrews [b], Ralph Nossal [c,*]

[a] *Reactor Radiation Division, National Institute of Standards and Technology, Gaithersburg, MD 20899, USA*
[b] *Physics Department, The College of Wooster, Wooster, OH 44691, USA*
[c] *Division of Computer Science and Technology, National Institutes of Health, Bethesda, MD 20892, USA*

Received 5 October 1993; accepted in revised form 15 April 1994

Abstract

The 30 m small angle neutron scattering facility at the National Institutes of Standards and Technology has been used to examine neutron scattering from agarose gels formed in D_2O. Differential scattering cross sections have been acquired over a continuous range of Q between 0.005 and 0.3 $Å^{-1}$. Subtle changes in gel structure are observed when pre-gelation agarose concentration is varied. Similarly, except when the gelling solution is rapidly cooled to a low temperature, the rate at which the gels are formed does not seem to have much effect. Clearer evidence of structural rearrangement is observed when the solvent quality is changed by the addition of dimethyl sulfoxide, or when the temperature of the gel is elevated above 70°C. These data are consistent with a description of a randomly structured polymer network containing discrete self-similar, hydrogen-bonded, junctions normally of minimal thickness $\approx$ 35–40 Å.

Keywords: Neutron scattering; Gels; Agarose

1. Introduction

Agarose has long been familiar to biochemists and molecular biologists as a matrix for electrophoretic separation of macromolecules. In particular, agarose-based pulsed gel electrophoresis is widely used for the separation and analysis of long fragments of DNA [1,2]. Yet, despite the great importance of agarose matrices in biotechnological applications, relatively little is known about their microstructure. Such information could be quite useful, because characteristics such as void size, strand thickness, gel microheterogeneity, and correlations in spatial structure – as well as changes that might occur when electric fields are applied [3,4] – can be expected to influence the way macromolecules migrate through such gels.

Although many useful separation procedures have been devised by empirical means, the development of increasingly complex electrophoretic separation procedures will be advanced by deeper understanding of the factors that determine how a gel functions as a separation matrix. However, this subject is complicated by the fact that a typical bulk gel is quite amorphous, so statistical methods are needed to define and characterize relevant structural attributes.

* Corresponding author.

SSDI 0301-4622(94)00079-Y

Furthermore, because gel matrices can be quite labile, care must be taken that the techniques used to study physical properties be minimally disruptive. Scattering methods allow non-invasive examination of gels and, although relatively large amounts of sample are required, both static and dynamic aspects of structure can be investigated. Several structural studies of agarose gels and closely related polysaccharide gels already have been carried out, in which methods of small angle light scattering (SALS) [5,6], small angle X-ray scattering (SAXS) [7,8], and small angle neutron scattering (SANS) [8,9] were utilized. These techniques probe somewhat different length scales and, to a certain degree, are sensitive to the presence of different atomic scattering centers. Studies of polyacrylamide gels have illustrated how coordinated observations involving all three techniques (SANS, SAXS, SALS) can be combined to give a continuous picture of structural fluctuations over a very wide range of length scales [10].

Here we report SANS measurements of the differential scattering cross-section, $I(Q)$, from a series of agarose gels. Measured cross-sections span a length scale from approximately 25 to 1200 Å, for which range the effects of such factors as polymer concentration, cooling rate, and solvent quality have been examined. Analogous SAXS data exist [7] for some of these experimental conditions. However, there is little direct overlap between our data and those acquired by small angle light scattering, as the latter mostly relate to structural information on a different length scale. We find, as a result of the present study, that SANS can probe properties of the junctional domains formed between individual agarose strands.

2. Methods and materials

2.1. Small angle neutron scattering

Data were acquired using the 30 m SANS instrument [11] located in the Cold Neutron Research Facility at the National Institute of Standards and Technology (NIST). The nominal neutron wavelength was 6.0 Å, with a spread of $\Delta\lambda/\lambda \approx 33\%$. Various instrument configurations were used, and the neutron beam in each case was collimated by adjusting the incident flight path, using neutron guide sections that can be moved into the beam to change the effective source-to-sample distance. Raw data were corrected for beam-blocked background counts and solvent absorbance and scattering according to the method of Chen and Bendedouch [12]. The data then were radially averaged to produce differential scattering cross sections $I(Q)$ as a function of Q, where $Q = 4\pi\lambda^{-1} \sin\theta$ and 2θ is the scattering angle. By varying the sample-to-detector distance and taking several overlapping sets of data, cross sections were measured over a wide range of Q with good precision ($0.005 \leqslant Q \leqslant 0.3$ Å^{-1}). Radially averaged cross sections measured at intermediate sample-to-detector distances were put on an absolute scale by calibration against the scattering from a silica-gel standard sample. Cross sections obtained from the same samples at other sample-to-detector distances were scaled to these data by matching amplitudes over appropriate overlapping regions of Q. Occasionally different, although nominally identical, samples were used when data were acquired at differing detector positions. Contributions arising from incoherent scattering by hydrogen in the agarose sample were estimated by measuring equivalent solutions of H_2O/D_2O (see Section 4).

Samples were contained in 2.0 or 3.0 mm path length cuvettes and normally were measured at 24 ± 1°C (room temperature). However, the sample stage could be heated and the temperature maintained to ±0.1°, and several measurements were made to investigate the effects of temperature on network structure and to discern changes that occur when a gel melts. In these studies, the sample was allowed to come to equilibrium at predetermined temperatures, which then were held constant while scattering data were accumulated.

2.2. Materials

Standard gels were prepared by first heating D_2O–agarose suspensions to 95°C in capped plastic conical centrifuge tubes. The resulting agarose solutions were kept at that temperature for several minutes and then rapidly placed into quartz scattering cuvettes. When preparing samples for a concentration series, hot agarose stock solution was diluted into appropriate amounts of hot D_2O.

Samples generally were allowed to cool in air at room temperature, during which time gelation occurred. To study the effects of quench rate on resulting gel structure, standard 3% (nominal) solutions also were cooled by rapidly immersing cuvettes filled with hot solution (a) into a 4°C ice bath and (b) into a circulating water bath maintained at various preset temperatures. Also, several samples were prepared in solvents that contained varying amounts of protonated (i.e. *non*deuterated) dimethyl sulfoxide (DMSO). In such cases agarose powder was suspended in premixed D_2O–DMSO solvents and the suspensions then were heated to 95°C as described above.

Unless otherwise indicated, the agarose used in these studies was identical to that used in earlier dynamic light scattering experiments [13]. This material, obtained several years ago from Kallestad Laboratories, Chaska, MN (Lot J011) but prepared by Marine Colloids (presently FMC BioProducts), has a gel strength break force of 977 g/cm^2 at 1% gel concentration. To add to our earlier familiarity with the properties of the gels which it forms, we further characterized this agarose powder by drying an aliquot in a 70°C oven and noting its weight change, from which we inferred that the powder sample contains approximately 12% water. Hence, all gel concentrations reported here are nominal values, and should be multiplied by a factor of 0.9 to obtain the true polymer weight concentration. Based on published product descriptions and differential scanning calorimetry measurements from which the gel points were determined to be $\approx$ 36–38°C (3% gels: 36.8 $\pm$ 0.5°C; 5% gels: 37.6 $\pm$ 0.5°C), we believe that this agarose has a medium electroendosmosis index and is similar to material that was marketed previously by Marine Colloids as SeaKem™ standard agarose.

Because agarose is obtained from mixtures of seawoods, different samples might contain different amounts of sulfate groups, pyruvate, or methoxyl content. These residues influence physical properties – especially residual charge – and consequently affect electrophoretic separations [14]. Agarose now is commercially available in several grades and we show here, as an example, that one such product – SeaKem™ Gold Agarose (FMC BioProducts, Rockland, ME) – has features in its scattering cross section which are qualitatively similar to those seen in our other samples. According to the manufacturer, the chemical and physical specifications of this sample (Lot No. 719892) are: gelling temperature (1.5%) 36 $\pm$ 1.5°C, moisture $\leqslant$ 10%, sulfate $\leqslant$ 0.10%, gel strength (1%) $\geqslant$ 1800 gm/cm^2, EEO ($-m_r$) $\leqslant$ 0.05.

3. Analysis and results

Scattering cross sections were measured for various agarose gels, the latter usually being prepared from the same material (see above) but under different conditions. Our 'standard' sample was a 3% (nominal) agarose gel formed in D_2O at room temperature. The major features of the SANS cross sections measured for this and similar samples are indicated schematically in Fig. 1. Three regions can be delineated: in region I, at small values of Q ($0.005 \leqslant Q \leqslant 0.025$ Å^{-1}, corresponding to a length scale $L = 2\pi Q^{-1}$ such that $250 \leqslant L \leqslant 1200$ Å), one observes $\log I(Q) \sim -\alpha \log Q$, i.e. $I(Q) \sim Q^{-\alpha}$; in region II, at larger values of Q, one finds *for usual D_2O solvent conditions* $I(Q) \sim Q^{-\beta}$, where $\beta > \alpha$; in region III, for $Q > 0.08$ Å^{-1} ($L < 80$ Å), one finds that $\log I(Q)$ is a slowly varying function of $\log Q$, appearing more-or-less 'flat' when compared with regions I and II. As discussed later, a significant portion of the weak scattering noted at high Q might be due to incoherent scattering from hydrogen which is introduced into the scattering system by the agarose itself. However, we shall see, below, that the values

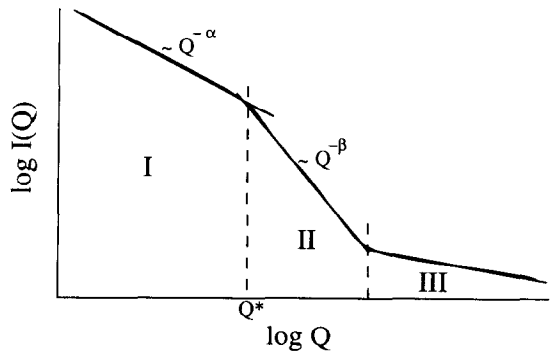

Fig. 1. Schematic diagram of the differential scattering cross section measured for normal agarose gels. The value Q^* changes when a gel is heated close to its melting point or when the solvent quality is changed.

of $I(Q)$ in region III change when a gel is heated or when certain other sample conditions are varied.

Several schemes have been used to interpret scattering data having the characteristics seen in regions I and II. Here we analyze our measurements in terms of a theory, first derived by Martin and Ackerson [15], and later elaborated upon by Bouchaud et al. [16]. This treatment is based on a model of uncorrelated compact fractal domains which, in the case of agarose gels, seem to be localized, net-like clusters (see Section 4). The theory indicates that the observed scattering intensity should behave as [15–17]

$$\begin{aligned} I(Q) &\sim Q^{-D(3-\tau)}, \quad \text{if} \quad \xi_0 Q \ll 1, \\ I(Q) &\sim Q^{-D}, \quad \text{if} \quad \xi_0 Q \gg 1, \end{aligned} \tag{1}$$

where the terms D, τ and ξ_0 signify the following: D is the mass fractal dimension of the domains, i.e. $R^D \sim M$; τ is the polydispersity index of the mass, where the mass distribution $P(M)$ is assumed to be given as $P(M) \sim M^{-\tau}$ [18,19]; ξ_0 corresponds to the 'radius of the smallest cluster' [8,17] (here assumed to be the minimal size of a junction domain). For a percolation model of gelation, $D = 2.5$, $\tau \approx 2.2$, and $D(3-\tau) \approx 2$ [19,20]. Other models (e.g., diffusion limited aggregation – DLA) also yield values of D close to 2.5, but give rise to somewhat different values of τ. We will see that Eq. (1) allows us to identify and rationalize the features shown in regions I and II of Fig. 1. In particular, the changes effected by variation of experimental conditions (e.g., concentration, temperature, and the nature of the solvent) can be readily explained (see Section 4).

3.1. Variation with gel concentration

In Fig. 2 we show the differential scattering cross section, $I(Q)$, for three values of agarose concentration. These samples, prepared in D_2O, were gelled at room temperature (≈ 24°C), the latter also being the temperature at which the scattering was measured. Several detector positions were employed in order to obtain data over such a wide range of Q, but the overlap noted in Fig. 2 was achieved without manipulation of the data other than described above in Section 2. The cross sections are plotted logarithmically on an absolute scale, as log $I(Q)$ versus log Q, over a range $0.005 \leqslant Q \leqslant 0.3$ Å^{-1}.

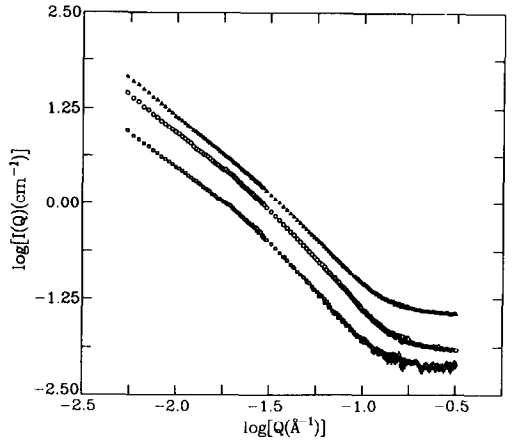

Fig. 2. log $I(Q)$ versus log Q for gels of differing agarose concentration. (□) 1% wt/vol; (○) 3% wt/vol; (△) 5% wt/vol.

We observe in Fig. 2 that, although the intensities scale with the concentration, all curves have the general form shown in Fig. 1. Each of the curves exhibits a slowly varying, but essentially constant, negative slope at small values of Q (region I), a clearly different slope at intermediate values (region II), and a leveling at higher Q values (region III). The slope in region II seems to be independent of the gel concentration, and is very close to a value $-\beta = -2.5$. In contrast, the slope in region I *does* vary somewhat with pre-gelation agarose concentration, being lower at lesser concentrations: For example, if one fits the slopes to the first 15 data points, i.e. $0.005 \leqslant Q \leqslant 0.011$, one finds $\alpha \simeq 1.78$ ($C = 1\%$), $\alpha \simeq 1.91$ ($C = 3\%$), $\alpha \simeq 1.97$ ($C = 5\%$); if one fits to the range $0.006 \leqslant Q \leqslant 0.019$, one finds $\alpha \simeq 1.82$ ($C = 1\%$), $\alpha \simeq 1.95$ ($C = 3\%$), and $\alpha \simeq 2.04$ ($C = 5\%$). We note that the value $\beta = 2.5$, seen in region II, is expected for structures whose connectivities are similar to those of threshold-percolation clusters [21]. The slopes in region I are close to the value $\alpha = 2$ which, according to Eq. (1), is consistent with a percolation model. The slight, but decreasing, variation of α with concentration may indicate that the junctional nets are, in effect, somewhat more swollen at lower agarose concentrations. Alternatively, such variation might arise from changes in large-scale structure of the gel network, particularly the increase in pore size noted as the concentration is lowered [22]. It may also be of interest that certain branched

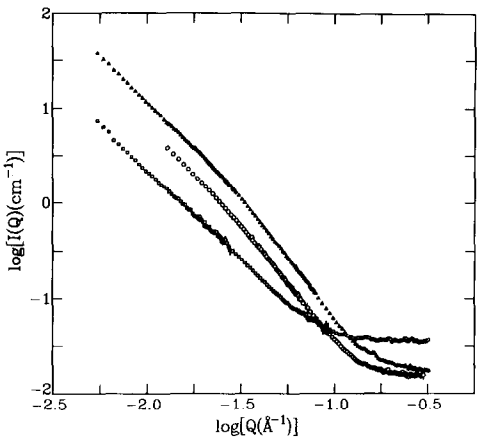

Fig. 3. log $I(Q)$ versus log Q for 3% agarose gels formed in D_2O–DMSO solvents. (△) 0% DMSO; (○) 10% DMSO; (□) 20% DMSO.

polymer structures yield values $\alpha \approx 2$ for relatively small Q, independent of the degree of branching and even when polymerizing to a gel [23].

3.2. Effects of solvent quality

If the model leading to Eq. (1) is correct, the breakpoint at the intersection between regions I and II, designated as Q^* in Fig. 1, might move if the junctions are modified. In Fig. 3 we show log $I(Q)$ versus log Q for agarose gels formed when DMSO is added to the solvent. DMSO disrupts hydrogen bonding in polysaccharide gels [24,25], so it is not surprising to see changes in the scattering cross section for values of Q where features associated with intrastrand bonding can be discerned. Note that the effect of DMSO is to extend the range where the slope is $\alpha \approx 2$ (region I). In fact, although for the 10% DMSO sample some residual of the $\beta = 2.5$ region remains, in the case of the 20% sample the region of steeper slope appears to vanish completely.

If it is assumed, in accord with Eq. (1), that the intersection of the extrapolated power law dependences of $I(Q)$ occur at $Q^*\xi_0 \approx 1$ (see Fig. 1), then the fact that $\xi_0 = (Q^*)^{-1}$ gets smaller as DMSO is added can be rationalized as indicating a disruption of hydrogen bonds between strands, leading to a thinning of the intrastrand junctions. In Fig. 2, where we show data for gels formed in pure D_2O, the break point Q^* occurs at a value of $Q^* \approx 0.025$–0.028 Å^{-1}, which would imply junctions of minimal thickness $\xi_0 \approx 35$–40 Å. It is quite interesting that this value is close to the value for typical fiber diameter, ≈ 50 Å, inferred many years ago by chromatographic methods [26].

It should be stressed that in this investigation we have used only protonated DMSO. The cross sections presented in Fig. 3 have been obtained by subtracting solvent scattering pertaining to each particular data set. However, because the contrast between the agarose strands and the solvent decreases as the amount of protonated DMSO is increased, there is a corresponding decrease in the amplitude of $I(Q)$ (relative to that of the silica-gel standard – see Section 4). This effect is seen clearly in the low Q region shown in Fig. 3. Significantly, though, despite the decrease in contrast occurring in the 20% DMSO sample, the scattering in the high Q region of that sample seems to *increase* by a factor of 2 (the ordinate in Fig. 3 is a logarithmic scale). (The change in contrast and small uncertainties in background corrections make it difficult to ascertain whether the intensities of the 0% and 10% DMSO samples differ in region III; the use of deuterated DMSO might enable one to draw conclusions about structural changes in this case as well.)

3.3. Effects of heating to the gel–sol transition

Another way to disrupt intrastrand bonding is to heat an agarose gel to temperatures near that at which solation occurs. In Fig. 4 we show log $I(Q)$ versus log Q for a standard 3% gel sample as it is heated from room temperature (≈ 24°C) to 95°C. The cross sections are identical for $T = 25$°C and $T = 40$°C. However, as expected, when the temperature approaches that of the melting point (which seems to be ≈ 65–70°C for this sample) the break point Q^* moves to larger values and the sharply decaying portion of the curve (region II) vanishes. When the temperature reaches $T = 95$°C the gel is solated, and the scattering cross section dramatically changes character. Instead of having the features seen in Fig. 1, log $I(Q)$ versus log Q in this instance is a smoothly varying curve which indicates, perhaps, a wide distribution of particles ('microgels'?) of relatively small size.

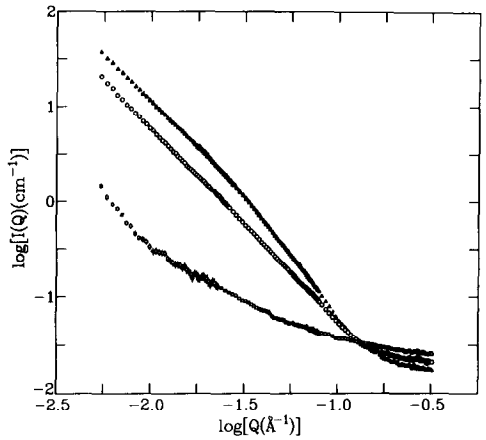

Fig. 4. log $I(Q)$ versus log Q for a standard 3% agarose gel as it is heated to its melting point. (△) 25°C; (▲) 40°C; (○) 70°C; (□) 95°C. (Note that the 25° and 40° data essentially superimpose.)

A particularly interesting feature of these curves, when taken as a group, is seen at large values of Q. As the gel is heated, the slowly varying portion of the curve (region III) increases in intensity. Although such changes might indicate the liberation of short agarose strands as the gel is heated, it is more likely that one is observing a decrease in steric correlations between molecular groups located within particular junctional regions. This indication of enhanced degrees of freedom of individual strands occurs concomitantly with a decrease in intensity of regions I and II of $I(Q)$ and, at the highest temperatures, the total disappearance of a well-defined region II.

Because for any given detector position the sample was not changed (only the temperature was varied), changes in the intensity of the flat portion of $I(Q)$ can *not* be ascribed to variable background corrections to the raw data. As already discussed, similar changes are observed in the data acquired to assess the effects of solvent quality (see the 20% DMSO data in Fig. 3). Also, it should be noted that the effects of heating are reversible. When the gel sample is allowed to cool after it has been heated to the point where solation has occurred, the cross section associated with $T = 25$°C and $T = 40$°C in Fig. 4 is recovered (data not shown). In particular, the latter observation is true for cross-sections measured at high Q (in region III).

3.4. Dependence on quench and cooling rate

It is known that the physical properties of agarose gels are only weakly dependent on the cooling rate to which a sol is subjected as it cools [14]. In Fig. 5 we show $I(Q)$ versus Q for several samples of identical 3% agarose concentration which differ only in that they were quenched at different rates when gelation was initiated. That is, after being filled with the same hot agarose solution, the cuvettes were either (a) placed in a circulating water bath held at room temperature, (b) cooled in air, or (c) placed in an ice bath. We note that the initial slopes of log $I(Q)$ versus log Q are indistinguishable, but the location of the break point Q^* varies a bit and the flat regions level off at distinctly different intensities. Hence it appears that the larger-scale structure may be relatively unaffected by quench and cooling rates, but the nature of the intra-junctional strand associations might be affected slightly. It should be noted that placing the samples in water baths of differing temperatures ($15 \leqslant T \leqslant 85$°C) seems to have even less effect, as the measured $\{I(Q)\}$ are virtually identical in each case (data not shown). As discussed previously, because separate samples were used, small variations seen here in the measured cross sections may be insignificant. However, the changes noted for the rapidly quenched specimen (ice water) probably indicate real differences between that sample and the others. For example, it is known that under certain circumstances agarose forms isolated strands of varying thicknesses [27,28], and there may be differences in the amount of agarose incorporated into the gel matrix of the rapidly quenched sample.

4. Summary and discussion

The main purpose of this work has been to identify those features of the differential scattering cross section that might indicate changes in the junctional regions of a network held together by self-associations of primary polymer strands. To do so, we selectively modified the conditions of preparation of agarose gels and thereby examined relations between gel structure and pre-gelation agarose concentration, the effects of quench and cooling rates, and changes

brought about by variations in solvent quality. By monitoring scattering as the sample temperature was raised and lowered, we also investigated structural changes related to the sol–gel transition.

Although various schemes have been proposed to analyze scattering data from amorphous polymer networks, we here used an analysis based on a model of a random distribution of compact self-similar junctions of arbitrary length but differing thicknesses. This model is suggested by observations that, within gels, agarose fibers of varying thicknesses form randomly structured clusters of relatively high density, resulting in the voids through which molecules move during electrophoresis [22,29]. Electron micrographs indicate that these clusters have net-like appearances, which seem to be randomly structured three-dimensional webs whose dimensions vary over a range from tens of angstroms (the thicknesses of individual strands) to several thousand angstroms [22]. The length scales of the structural features of such junctions clearly lie within the region probed by our SANS measurements. At that level, the random, reticulate form of the junctions resembles that of other structures which have been described as having fractal characteristics.

This treatment differs a bit from other methods used to analyze SANS and SAXS data from agarose gels which consider the sample to be composed of a sparse, discrete population of rod-like aggregates [7] or a random network of bundles of rod-like molecules [9]. Indeed, experiments on the sieving of spheres of known dimensions indicate that a model of gel composed of straight randomly oriented fibers is inappropriate [29,30]. We favor the model of a random assembly of condensed net-like junctions because of its ability to account for the most prominent feature of the measured $\{I(Q)\}$, viz., the almost discontinuous change in slope of log $I(Q)$ versus log Q at a value of $Q^* \approx 0.025$–0.028 Å^{-1}. Also, the model is in qualitative agreement with the changes in cross-section which are observed as experimental conditions are varied.

We tried to design the protocols of this study to take into account various intrinsic limitations of the SANS technique. For example, the wavelength spread of the SANS spectrometer results in relatively poor resolution at high values of Q. Also, incoherent scattering from the hydrogen in the native agarose molecules contributes to the background so, at higher values of Q, the ratio of signal to noise is rather low.

The latter point requires further commentary. An approximate calculation of the amount of hydrogen in a typical, nominally 3%, wt/vol agarose sample can be carried out by noting that the standard agarobiose repeating unit contains 12 carbon, 9 oxygen, and 18 hydrogen atoms. Hence, the weight fraction of hydrogen in the molecule is $18/309 = 0.059$, so a 3% sample contains 0.0018 gm/cc hydrogen. The presence of bound water, sulfate groups, etc. does not significantly change this estimate (i.e. ≈ 0.002 gm/cc H^+), which also is approximately the amount of H^+ present in a 2% H_2O in D_2O sample. We therefore measured the absolute scattering cross section due to a 2% H_2O–98% D_2O sample and found it to be ≈ 0.088 cm^{-1} in the high Q region, as compared with a corresponding value of 0.068 cm^{-1} for a nominally 100% D_2O sample. In this way the incoherent background arising from H^+ in the agarose is estimated to be approximately 0.02 cm^{-1}, which is close to the levels discerned in region III for our 'standard' 3% agarose samples ($\log_{10}(0.02) = -1.7$).

This intrinsic incoherent scattering makes it difficult to infer details of structure from features of $I(Q)$ at higher values of Q. Although one might wish to subtract the incoherent scattering associated with the agarose, the latter can be determined only imprecisely. However, because the amplitude of the background is several orders of magnitude less than reported values of $I(Q)$ in regions I and II, any proper background subtraction would leave those values essentially unaffected. (The slopes of log $I(Q)$ versus log Q typically change by only a few percent.) We also note that, because the data follow power laws in regions I and II, the effects of collimation and wavelength smearing on the resolution in those regions can be easily tested by simple computations. These indicate that smearing under our experimental conditions causes only inconsequential increases of approximately 1% in the values of α and β.

In region III, where the background level is significant, principal interest is in the variations of cross-section noted as experimental conditions are changed, if the amount of incoherent scattering is kept constant. When the temperature was varied, the

same sample was used throughout the study. Thus, changes in $I(Q)$ noted at high Q (see Fig. 4) can be ascribed to changes in the status of the agarose constituents. In a like manner the data shown in Fig. 5 – on the effects of cooling rate during gel formation – were obtained for samples produced from the same hot agarose solution. The samples in that series therefore contained identical concentrations of hydrogen. (The constancy of the incoherent scattering is borne out by the fact that the measured transmissions of all of the 3% samples were identical, whatever the temperature or the quench conditions.) We note, also, that background scattering by the solvent was subtracted [12] for each of the DMSO cross-sections shown in Fig. 3, which mitigates against the DMSO being a significant source of H^+. For these reasons we believe that the changes noted in the high Q region of $I(Q)$ almost certainly represent changes of the agarose matrix.

We find that our inferred model of compact fractal junctional domains is consistent with qualitative inferences drawn from electron micrographs [22]. However, it is expected that the preparation of samples for electron microscopy may lead to changes in the three dimensional structure of the polymer matrix. Fixation artifacts probably limit the use of electron microscopy for quantitative study of the various factors that influence network characteristics.

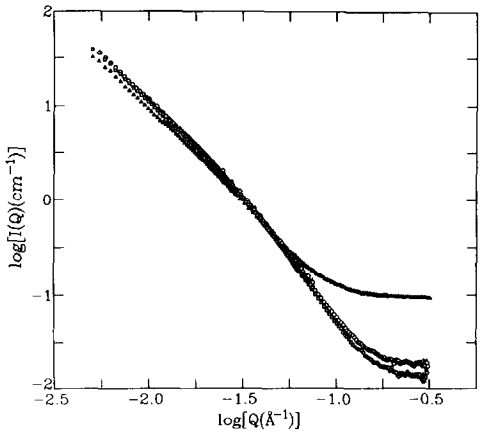

Fig. 5. log $I(Q)$ versus log Q for standard 3% agarose gels quenched at different rates after gelation was initiated. (△) 4°C water bath; (○) 25°C water bath; (□) cooled in air at room temperature.

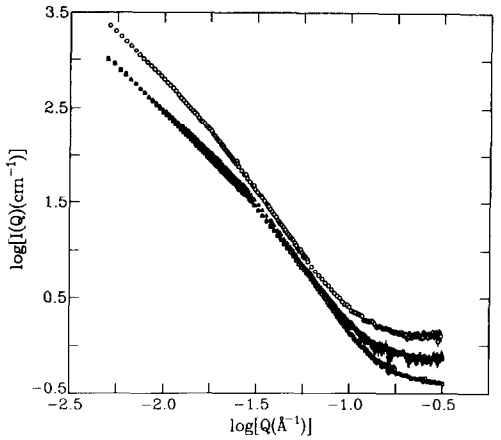

Fig. 6. Scattering cross-sections for gels of different concentration (cf. Fig. 2), here the scattering intensities have been rescaled according to the discussion in the text. (○) 1.5% SeaKem™ Gold gel; (▲) 5% standard gel; (□) 3% standard gel; (△) 1% standard gel.

Hence, it may be that relationships between solvent quality and agarose gel structure are more reliably determined by non-invasive methods such as those afforded by SANS and other scattering techniques.

In Fig. 6 we again show the data which previously were presented in Fig. 2. Here, however, we have normalized the data to correspond to that of our standard 3% sample; that is, the scattering intensities obtained for the $C = 1\%$ sample were multiplied by 3 and the scattering intensities for the $C = 5\%$ sample were multiplied by the factor $\frac{3}{5}$. We see that the three curves nearly superimpose, differing primarily in the slopes in region I at smaller Q. For comparison, we also show similarly normalized data for a $C = 1.5\%$ gel formed from SeaKem™ Gold agarose (see Section 4). These data have been plotted without accounting for the fact that this sample probably contains less bound water than does the 'standard' powder sample. Therefore, the factor needed to obtain the true polymer concentration is higher than for the other samples and the data do not superimpose with the other curves. When such corrections are made, the absolute magnitudes of all of the concentration adjusted curves are quite similar. The principal point is that, although Q^* occurs at a slightly different value for the SeaKem™ Gold sample, the curves have the same overall shape despite the dif-

ference in sample identity and preparation. A sharp break in the slope has been noted, also, in other SANS studies of agarose [9] and in SAXS studies of certain κ-carrageenate gels [8]. Similar characteristics have been seen in SANS studies of poly (vinyl alcohol)-borate gels [17] and silica particle aggregation [31]. In contrast, studies of gels of steroid/hydrocarbon organogels, which consist of aggregates of rigid rods, yield very different features [32].

Other investigators, using SAXS, have inferred that structural features remain invariant when agarose concentration is changed [7]; however, because our SANS studies examine scattering in a range of Q that extends to a somewhat smaller values than were accessible in the earlier SAXS studies, we discern previously unnoticed structural changes, on the order of 250 Å and greater, as the concentration is varied. Although structural features at smaller distances do not seem to be affected by changes in concentration, they are indeed influenced by changes in solvent quality. Having identified these features, we now should be able to use SANS to extend, to smaller length scales than previously probed [3,4], structural studies of changes in gel microstructure that might be brought about by the imposition of electric fields. We also expect to be able to use these methods to investigate junction formation in other rod-like biopolymer networks [33].

Acknowledgement

The authors thank Dr. Boualem Hammouda for his generous and insightful participation in several important discussions. We also thank Dr. Fred Schwarz for performing the differential scanning calorimetry measurements mentioned, above, in Section 2. Support for this work was provided in part by the National Science Foundation under agreement No. DMR-9122444. Note: Certain trade names and company products are mentioned in the text or identified in an illustration in order to adequately specify the experimental procedure and equipment used. In no case does such identification imply recommendation or endorsement by the National Institute of Standards and Technology, nor does it imply that the products are necessarily the best available for the purpose.

References

[1] C.R. Cantor, C.L. Smith and M.K. Mathew, Ann. Rev. Biophys. Biophys. Chem. 17 (1988) 287–304.
[2] M. Burmeister and L. Ulanovsky, eds., Methods in molecular biology, Vol. 12, Pulsed-field electrophoresis (Humana Press, Totowa, 1992).
[3] J. Stellwagen and N.C. Stellwagen, Nucleic Acids Res. 17 (1989) 1537–1548.
[4] N.C. Stellwagen and J. Stellwagen, Electrophoresis 14 (1993) 355–368.
[5] E. Pines and W. Prins, Macromolecules 6 (1973) 888–895.
[6] P.L. San Biagio, F. Madonia, F. Sciortino, M.B. Palma-Vittorelli and M.U. Palma, J. Phys. (Paris) 45-C7 (1984) 225–233.
[7] M. Djabourov, A.H. Clark, D.W. Rowlands and S.B. Ross-Murphy, Macromolecules 22 (1989) 180–188.
[8] K. Kajiwara, S. Kohjiya, M. Shibayama and H. Urakawa, in: Polymer gels. Characterization of gel structure by means of SAXS and SANS, eds. D. DeRossi, K. Kajiwara, Y. Osada and A. Yamauchi (Plenum Press, New York, 1991) p. 3–19.
[9] A. Deriu, F. Cavatorta, D. Cabrini and H.D. Middendorf, Progs. Colloid Polym. Sci. 84 (1991) 461–464.
[10] A.-M. Hecht, R. Duplessix and E. Geissler, Macromolecules 18 (1985) 2167–2173.
[11] B. Hammouda, S. Krueger, and C.J. Glinka, J. Res. Nat. Inst. Stand. Technol. 98 (1993) 31–46.
[12] S.-H. Chen and D. Bendedouch, Methods Enzymol. 130 (1986) 79–116.
[13] S.L. Brenner, R.A. Gelman and R. Nossal, Macromolecules 11 (1978) 202–207;
R. Nossal and M. Jolly, J. Appl. Phys. 53 (1982) 5518–5525.
[14] F.H. Kirkpatrick, M.M. Dumais, H.W. White and K.B. Guiseley, Electrophoresis 14 (1993) 349–354.
[15] J.E. Martin and B.J. Ackerson, Phys. Rev. A 31 (1985) 1180–1182.
[16] E. Bouchaud, M. Delsanti, M. Adam, M. Daoud and D. Durand, J. Phys. (Paris) 47 (1986) 1273–1277.
[17] M. Shibayama, H. Kurokawa, S. Nomura, M. Muthukumar, R.S. Stein and S. Roy, Polymer 33 (1992) 2883–2890.
[18] D. Stauffer, Phys. Rept. 54 (1979) 1–74.
[19] J.E. Martin, J. Appl. Cryst. 19 (1986) 25–27.
[20] A. Aharony, Fractal growth, in: Fractals and disordered systems, eds. A. Bunde and S. Havlin (Springer, Berlin, 1991) pp. 152–173.
[21] D.W. Schaefer. C.J. Brinker, D. Richter, B. Farago and B. Frick, Phys. Rev. Letters 64 (1990) 2316–2319.
[22] G.A. Griess, K.B. Guiseley and P. Serwer, Biophys. J. 65 (1993) 138–148.
[23] D.W. Schaefer and K.D. Keefer, Phys. Rev. Letters 53 (1984) 1383–1386.
[24] M. St-Jacques, P.R. Sundararajan, K.J. Taylor and R.H. Marchessault, J. Am. Chem. Soc. 98 (1976) 4386–4391.
[25] Q. Peng and A.S. Perlin, Carbohydr. Res. 160 (1987) 57–72.
[26] T.C. Laurent, Biochim. Biophys. Acta 136 (1967) 199–205.
[27] Y. Dormoy and S. Candau, Biopolymers 31 (1991) 109–117.

[28] J.-M. Guenet, A. Brûlet and C. Rochas, J. Biol. Macromol. 15 (1993) 131–132.
[29] G.A. Greiss and P. Serwer, Proc. Electron. Microscopy Soc. Am. 57 (1989) 884–885.
[30] G.A. Greiss, E.T. Moreno, R.A. Eason and P. Serwer, Biopolymers 28 (1989) 1475–1484.
[31] T. Freltoft, J.K. Kjems, and S.K. Sinha, Phys. Rev. B 33 (1986) 269–275.
[32] P. Terech, J. Phys. (Paris) 50 (1989) 1967–1982.
[33] D.H. Wachsstock, W.H. Schwarz and T.D. Pollard, Biophys. J. 65 (1993) 205–214.